Template-Free Liquid-Phase Synthesis of High-Density CdS Nanowire Arrays on Conductive Glass

ARTICLE *in* THE JOURNAL OF PHYSICAL CHEMISTRY C · JANUARY 2009

Impact Factor: 4.77 · DOI: 10.1021/jp809365z

5 AUTHORS, INCLUDING:

Sung-Hwan Han
Hanyang University
336 PUBLICATIONS **5,205** CITATIONS
SEE PROFILE

Yun-Mo Sung
Korea University
107 PUBLICATIONS **1,646** CITATIONS
SEE PROFILE

Article

Template-Free Liquid-Phase Synthesis of High-Density CdS Nanowire Arrays on Conductive Glass

Woo-Chul Kwak, Tae Geun Kim, Wonjoo Lee, Sung-Hwan Han, and Yun-Mo Sung

J. Phys. Chem. C, **2009**, 113 (4), 1615-1619 • DOI: 10.1021/jp809365z • Publication Date (Web): 07 January 2009

Template-Free Liquid-Phase Synthesis of High-Density CdS Nanowire Arrays on Conductive Glass

Woo-Chul Kwak,[†] Tae Geun Kim,[‡] Wonjoo Lee,[§] Sung-Hwan Han,[§] and Yun-Mo Sung*[,†]

Department of Materials Science and Engineering, Department of Electronic Engineering, Korea University, Seoul 136-713, South Korea, and Department of Chemistry, Hanyang University, Seoul 133-791, South Korea

Received: October 22, 2008; Revised Manuscript Received: December 17, 2008

High-density and single-crystalline CdS nanowire arrays were formed on fluorine-doped tin oxide (FTO)-coated soda-lime glass substrates without aid of templates at 220 °C. Bi was employed as a catalyst for the low-temperature growth of CdS nanowires via solution−liquid−solid (SLS) mechanism. CdS nanowires were very straight and they were ∼20−50 nm in diameter and ∼2−3 μm in length. CdS nanowires were in highly crystalline wurtzite structure, and their crystal growth direction was [001]. Careful controlling of processing conditions including Bi catalyst size, precursor concentration, and processing temperature was effective to grow thin CdS nanowires by suppressing formation of nanoparticles and radial growth of nanowires. Poly vinyl alcohol (PVA) film covering Bi catalyst layer played a critical role in holding Bi liquid droplets on the substrates during nanowire growth. The potential of CdS nanowire arrays on FTO/glass substrates was demonstrated to be used for organic−inorganic hybrid solar cells.

1. Introduction

Recently semiconductor nanowires have attracted a great deal of attention due to their superior optical, electrical, and chemical properties compared to traditional bulk and thin film semiconductors, arising from defect-free single crystallinity, size confinement, increased surface-to-volume ratio, and so on.[1] Furthermore, nanoscale devices having highly sensitive signal transduction and increased integrated density can be tailored using semiconductor nanowires. Hence, they have demonstrated strong potential to be used for high-performance light-emitting devices, photodetectors, sensors, transistors, photovoltaics, electrodes, etc.[2] The synthesis routes of semiconductor nanowires can be roughly classified into two categories, vapor-phase growth[3] and liquid-phase growth.[4] In general, vapor-phase synthesis allows the growth of high-crystallinity and high-density nanowires, and it also allows formation of nanowire array patterns on a substrate. Yang et al.[5] nicely formed vertically grown single crystalline ZnO nanowire arrays on a sapphire substrate, and they demonstrated strong lasing from nanowire arrays. The top and bottom (001) basal planes of nanowires acted as mirror planes for lasing.

Buhro et al.[6] have reported successful liquid-phase synthesis, for instance solution−liquid−solid (SLS) growth of various nanowires. They produced high-quality semiconductor nanowires using a mild chemistry condition and demonstrated the advantages of using it to produce nanowires. However, liquid-phase synthesis generally produces nanowires freely dispersed in a solution instead of nanowires grown on a substrate. Many research groups tried to grow arrayed nanowires directly on a substrate using template-assisted methods. Anodic aluminum oxide (AAO) and polymer templates containing one-dimensional nanoscale channels were used for the liquid-phase synthesis of nanowire arrays on substrates.[7] Although this is a relatively easy method, the nanowires grown by template-assisted methods suffer from low crystallinity and they are mostly polycrystalline. Hence, their optical and electrical properties are not satisfactory compared to single crystalline nanowires grown by vapor-phase synthesis. Furthermore, nanowire arrays are collapsed and aggregated after removing templates and thus individually separated nanowire structures cannot be obtained, which can cause serious deterioration in physical properties, and the formation of nanoscale heterostructures or hybrids is impossible.

As mentioned above, mild chemistry can be employed for liquid-phase synthesis of nanowires at low temperature, and it is highly beneficial to form nanowire arrays vertically grown on a substrate. Owing to low-temperature mild chemistry, low-cost substrates such as soda-lime glass and even polymer can be used as substrates for nanowire growth. Also, nanowire growth on very wide substrates is possible in contrast to vapor-phase growth that is limited by the volume of a deposition chamber. Furthermore, transparent electronic devices such as solar cells can be designed based on nanowire-on-glass structures. Recently Park et al.[8] reported the synthesis of CdS/CdSe heterostructured nanowires on Si substrates via SLS growth. Although the nanowire growth was successful and individual CdS/CdSe nanowires revealed transistor behavior, nanowires grew almost parallel to the surface of Si substrates and thus device fabrication using nanowire arrays seems impossible. It is still challenging to fabricate highly crystalline nanowire arrays vertically grown on a substrate using liquid-phase synthesis.[9] In this study, we for the first time report template-free liquid-phase growth of CdS nanowire arrays on a substrate. High-density and single crystal CdS nanowires were successfully grown on fluorine-doped tin oxide (FTO), a transparent conducting oxide (TCO), coated soda-lime glass substrates at 220 °C via SLS mechanism. The growth mechanism for CdS nanowires was discussed in detail. Also, their potential to be used as photovoltaic cells was demonstrated by forming poly(2-ethynyl-*N*-carboxypropylpyridiniumperchlorate) (LM 4)-CdS nanowire hybrid solar cells.

* To whom correspondence should be addressed. E-mail: ymsung@korea.ac.kr. Tel: 82-2-3290-3286. Fax: 82-2-928-3584.
[†] Department of Materials Science and Engineering, Korea University.
[‡] Department of Electronic Engineering, Korea University.
[§] Department of Chemistry, Hanyang University.

10.1021/jp809365z CCC: $40.75
Published on Web 01/07/2009

2. Experimental Section

For the synthesis of CdS nanowires, 0.05 mmol of cadmium oxide (99.99%), 0.5 mL of oleic acid, 20 mg of hexadecylamine (98%), 150 mg of trioctylphosphine oxide (TOPO, 99%), and 8 mL of 1-octadecene (ODE) (Aldrich Chemical, Milwaukee, WI) were loaded in a 100 mL three-neck flask. The solution was heated to 220 °C under Ar flowing with stirring. CdS layer with ~40 nm thickness was deposited onto fluorine-doped tin oxide (FTO) substrates by DC sputtering. Subsequently, Bi thin layer with ~5 nm thickness was coated on the CdS layer by DC sputtering. Then glass substrates bearing Bi catalyst layer were dipped into poly(vinyl alcohol) (PVA) solution to produce PVA protection layer on the Bi catalysts. The PVA layer was employed to hold Bi catalysts on the substrates until the initiation of the CdS nanowire growth. Otherwise, we always loose the Bi catalyst and we cannot synthesize CdS nanowire via SLS method. The PVA/Bi/CdS/FTO/soda-lime glass substrates were heat treated at 250 °C under Ar flow in a tube furnace to break Bi layer into Bi nanoparticles serving as catalysts for the nucleation of CdS nanowires. After substrates bearing Bi catalysts were loaded into the flask containing the prepared solution, 0.5 mL of 5 wt % sulfur-tertiary butyl phosphine (TBP) solution was additionally injected into the solution, and the reaction was continued for 4 h under gentle stirring. The solution was cooled to room temperature, and resulting samples were rinsed with chloroform.

The crystal structure of CdS nanowires was investigated by X-ray diffraction (XRD, Rigaku Model D/MAX-2500V/PC, λ = 1.5418 Å). Field emission scanning electron microscopy (FESEM, Hitachi S-4300) was employed to examine the morphological feature of nanowires. High-resolution transmission electron microscopy (HRTEM, JEM 2100F, 200 kV) was used to examine crystallinity, and selected area electron diffraction (SAED) was conducted to confirm crystalline structure. UV−vis light absorption (Varian, CARY100) and photoluminescence (PL, Hitachi F-4500, Tokyo, Japan) were conducted on CdS nanowires to identify light absorption and emission properties.

The polymer photosensitizer was formed on nanowire arrays by in situ polymerization method that was carried out via the direct polymerization of 2-ethynylpyridine on CdS surface in ethyl acetate solution. CdS nanowire arrays grown on FTO glass substrates were immerged into 0.1 M 4-bromo-buyric acid in methanol solution at room temperature for 16 h and then polymerized with 2-ethynylpyridine in ethyl acetate (0.01 M for 24 h at 80 °C). The counterion of poly(2-ethynyl-*N*-carboxypropylpyridinium bromide) was ion-exchanged with 0.01 M sodium perchlorate/methanol. The poly(3-hexylthiophene) (P3HT) was layered by spin-casting and thermal deposition of Au electrode (~100 nm) followed. The polymer/CdS nanowire hybrids were characterized using UV−vis absorption spectroscopy (Varian, CARY100). The emission spectra of LM 4 and in situ polymerized LM 4/CdS on FTO were measured according to excitation wavelength (Photon counting spectrometer, ISS Inc.). LM 4 on FTO was prepared by spin-coating. $J-V$ characteristics were measured with a Kiethley 2400 source meter in the dark and under illumination from a 450 W xenon lamp (Oriel Instruments). The incident photon-to-current conversion efficiency (IPCE) was measured with respect to a calibrated Melles−Friot silicon diode (Photon counting spectrometer, ISS Inc. and Kiethley 2400 source meter) without bias illumination.

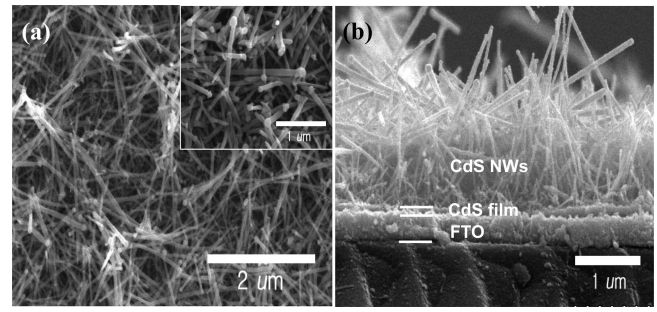

Figure 1. Field-emission scanning electron microscopy (FESEM) (a) top view and (b) cross-sectional view images of CdS nanowires grown on FTO/soda-lime glass substrates. The inset is the blown-up image showing Bi catalysts at the tip of nanowires.

3. Results and Discussion

CdS nanowires were synthesized on CdS/FTO/soda-lime glass substrates at 220 °C for 4 h by liquid-phase growth. The CdS layer was deposited on FTO for the purpose of obtaining homoepitaxial growth of CdS nanowires and overcoating FTO bottom electrodes. The high crystallinity of samples was confirmed using X-ray diffraction (XRD) (see Supporting Information). The XRD data indicate that nanowires have diffraction patterns corresponding to hexagonal (wurtzite) phase of CdS (JCPDS No. 80-0006). The relative diffraction peak intensity of CdS nanowires was different from the JCPDS data for polycrystalline CdS. The relative intensity of the (002) diffraction of nanowires was much higher than that from standard CdS powder, implying that CdS nanowires were grown into [001] direction (*c*-axis) and nanowires were preferentially aligned to one direction on a substrate rather than randomly oriented. Diffractions from FTO (101), (200), and (211) (JCPDS No. 88-0287) were also observed in XRD patterns.

Morphological features of samples were investigated by field emission electron microscopy (FESEM) analyses as shown in Figure 1. The average diameter and the length of nanowires grown at 220 °C for 4 h were ~40−80 nm and ~2−3 μm, respectively (Figure 1a). The small diameter of CdS nanowires should attribute to the small size of Bi catalysts. The breakage of thin Bi layer (~5 nm) can produce nanoscale Bi catalysts for SLS growth of nanowires. High-magnification FESEM image of samples (inset in Figure 1a) reveals that CdS nanowires are uniform and straight. Bi catalyst nanoparticles were readily observed at the tips of nanowires, confirming that SLS is the mechanism for nanowire growth. The mean diameter of CdS nanowires was found to be roughly 20−30% smaller than the mean size of Bi catalysts, which is probably due to low concentration of Cd and S precursors penetrating into bismuth catalysts by low-temperature synthesis. Cross-sectional FESEM image (Figure 1b) shows that CdS nanowires grew from the CdS/FTO layer with strong bonding. The CdS buffer layer played a major role in the growth of high-quality and high-density CdS nanowires. The samples without CdS buffer layer showed low-quality and low-density nanowire growth most probably due to the lattice mismatch between CdS and FTO. FTO has tetragonal rutile structure, while CdS has hexagonal wurtzite structure. So, there is very low probability to obtain favorable nucleation and growth of CdS nanowires on FTO layer. Although we used CdS buffer layer for homoepitaxial growth, the growth direction of nanowires was not perfectly vertical probably due to low crystallinity of predeposited CdS buffer layer and surface roughness of CdS/FTO layer. These two factors could cause weak epitaxial growth and tilted growth

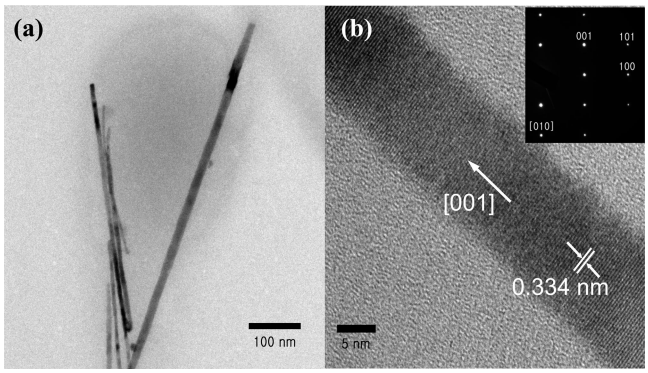

Figure 2. (a) TEM and (b) HRTEM images of CdS nanowires grown on FTO/soda-lime glass substrates. The inset is SAED pattern.

of CdS nanowires instead of strong vertical growth. Increase in the crystallinity and smoothness of CdS/FTO layer will further increase the degree of vertical growth of CdS nanowires.

Figure 2a shows that a low magnification TEM image of CdS nanowires detached from the CdS/FTO/soda-lime glass substrates of very straight and uniform diameter CdS nanowires was confirmed. Figure 2b presents a high-resolution TEM image of CdS nanowires showing clear lattice fringes. The interplanar *d*-spacing was 3.34 Å, indicating that the nanowire growth direction was [001], which is in good agreement with the XRD results. The selected area electron diffraction (SAED) patterns were indexed as the inset in Figure 2b, and they also confirm that a single crystalline wurtzite structure formed and the nanowire growth direction was [001]. Although nanowires were produced by a low-temperature liquid-phase process, they show high crystallinity without crystalline defects such as stacking faults.

The formation mechanism of arrayed nanowires through liquid-phase synthesis was proposed in Scheme 1. There are two important factors to be considered in our successful growth of arrayed CdS nanowires on glass substrates. First, most of Cd and S precursors should be consumed only for nanowire growth. Once CdS nanocrystals dominantly form in a solution by supersaturation of a precursor-bearing solution, only a few numbers of CdS nanowires could be found because of consumption of precursors by the nucleation and growth of nanocrystals. To suppress the nucleation and growth of nanocrystals, we took special care to control both precursor concentration and temperature of the solution. In general, the nucleation of crystals can be controlled by the driving force for the nucleation. Equation 1 describes the driving force for the bulk nucleation of crystals in a liquid solution.[10]

$$\Delta G_v = -\frac{kT}{\Omega}\ln\left(\frac{C}{C_o}\right) \quad (1)$$

where ΔG_v is the Gibbs free energy change during the nucleation of nanoparticles, C is the concentration of precursors, C_o is the equilibrium concentration, k is the Boltzmann constant, T is the temperature, and Ω is the atomic volume. The driving force for the nucleation is the decrease in the Gibbs free energy (ΔG_v) of the solution by precipitation of nuclei. According to eq 1, when C is higher than C_o (supersaturation), ΔG_v becomes a negative value and nucleation of nanoparticles occurs spontaneously. We maintained concentrations of Cd and S precursors as low as 0.0059 and 0.069 M, respectively, to prevent nucleation of CdS nanocrystals. Also, strong tendency to longitudinal growth of nanowires can be obtained at a low precursor concentration by suppressing radial (lateral) growth. Fast longitudinal growth is desirable for the growth of high-quality nanowires. According to following Gibbs−Thomson equation (eq 2), small radius (r) nanowires have high equilibrium concentration (C_c) at the curved surface, and this high equilibrium concentration can play a critical role in repelling precursors at the surface, resulting in preventing radial growth of nanowires.[11]

$$\ln\left(\frac{C_c}{C_\infty}\right) = \frac{2\gamma\Omega}{kTr} \quad (2)$$

where C_c is the precursor concentration at the curved surface of nanowires, C_∞ is the precursor concentration at the flat surface, γ is the surface energy, Ω is the molar volume, k is the Boltzman constant, T is the reaction temperature, and r is the radius of nanowires. Therefore, small diameter (40∼80 nm) of CdS nanowires, resulting from small size of Bi catalysts and low concentration of precursors penetrating the catalysts, can build up high local equilibrium concentration (C_c) at the surface, which is effective to prevent radial growth of nanowires by repelling precursors. Even though the initial diameter of CdS nanowires is small enough to create high equilibrium concentration (C_c) at the surface as presented in eq 2, when the precursor concentration in a solution is too high to exceed the local equilibrium concentration (C_c), negative concentration gradient occurs from the solution to the surface of nanowires and radial growth as well as longitudinal growth of nanowires can occur simultaneously. Thus, to suppress radial growth the precursor concentration of the solution should be maintained lower than local equilibrium concentration (C_c) at the surface.

Also, high T of a solution gives a more negative value of ΔG_v in eq 1 that corresponds to higher driving force for nucleation of nanocrystals. Thus, in this study the synthesis was conducted at a very low temperature of 220 °C, which reduces the driving force for the nucleation of CdS nanocrystals. Although both concentration and reaction temperature were low, the formation of Bi−Cd−S liquid-phase solution droplets was possible probably due to very low melting temperature (271 °C) of Bi. Since the Bi catalysts are in nanometer scale, their actual melting temperature could be lower and also the eutectic reaction between Bi and Cd/S precursors can further decrease the melting temperature to 146 °C.[12] Thus, the processing temperature of 220 °C was a temperature high enough to make liquid-phase Bi droplets as catalysts for the SLS growth of CdS nanowires. Spherical morphology of Bi catalysts existing at the tips of as-grown CdS nanowires as shown in Figure 1a is an evidence for formation of liquid-phase Bi droplets during the reaction.

Second, in order to obtain CdS nanowire arrays vertically grown from glass substrates, Bi catalyst layers were overcoated with PVA by dip coating. PVA could ensure adhesion of Bi catalysts to substrates during the nucleation and growth reaction. Without PVA coating, Bi catalysts disappeared from the substrates, and as a result CdS nanowires could not grow on the glass substrates. The wetting of Bi liquid droplets to the surface of glass substrates could be weak due to low processing temperature, and stirring and convection occurring in the solution can detach Bi liquid droplets from the glass substrates. At the initial stage of reaction, Cd and S sources reach Bi catalysts through the PVA layer and then adsorption and decomposition process occurs simultaneously. Once Bi liquid droplets supersaturate, CdS crystals nucleate at the interfacial regions between Bi catalysts and a glass substrate, and subsequently nanowires start to grow from the glass substrates.

SCHEME 1: Schematic Showing the Solution−Liquid−Solid (SLS) Growth of CdS Nanowires on FTO-Coated Soda-Lime Glass Substrates Using Bi Catalysts and PVA

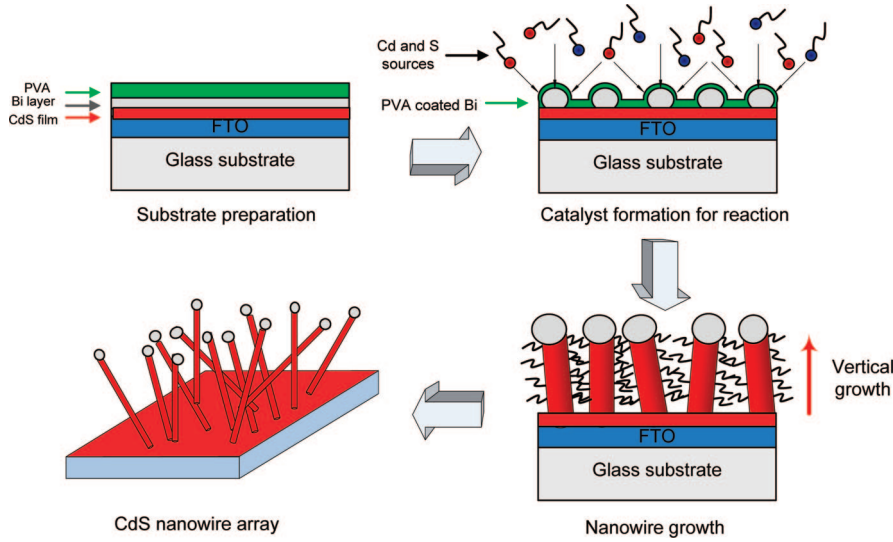

The procedure for the CdS nanowire growth on conductive oxide layer-coated glass substrates is depicted in Scheme 1.

UV−vis absorption spectra of as-prepared CdS nanowires show absorption peak at the wavelength (488 nm) corresponding to the energy band gap (2.54 eV) of bulk CdS (see Supporting Information). Slight red shift occurring in photoluminescence (PL) peak compared to the UV−visible peak attributes to the Stoke's shift. Strong PL intensity could come from high density and high crystallinity of CdS nanowires, which is contradictory to other liquid-phase synthesized nanowires showing poor PL intensity due to low crystallinity. The yellow luminescence possibly occurring due to crystalline defects was almost negligible in our CdS nanowires.

CdS nanowire arrays were dip coated with LM 4 polymer to form organic−inorganic hybrids. CdS nanowires with LM 4 coating was measured for UV−visible light absorption and they were compared with bare CdS nanowires prior to coating and LM 4 only, respectively in Figure 3a. Maximum UV−visible absorption peak of LM 4/CdS hybrids occur at around 503 nm, which is close to the band gap of LM 4 ($E_g \sim 2.46$ eV) indicating that LM 4 polymer is a light absorber in the hybrids. LM 4-CdS hybrids show an apparent increase in the visible light absorption compared to LM 4 polymer in the range of ~400 to ~600 nm due to the contribution of CdS. As shown in Figure 3b, PL emission was quenched in LM 4-CdS hybrids compared to LM 4 due to the effective electron and hole separation between LM 4 and CdS which is desirable for solar cell applications.

Hybrid photovoltaic cells were fabricated by constructing a CdS-LM 4-P3HT structure and a schematic diagram of its band structure is shown in Figure 4a. Cyclic voltammetry (not shown) and UV−vis spectroscopy measurements showed that the lowest unoccupied molecular orbital (LUMO) levels for LM 4 was −3.42 eV in vacuum.[13] The electrons excited to the LUMO of the polymers can transfer into the conduction band of CdS (−4.2 eV). The functional group in the conjugated polymer photosensitizers has strong linking to CdS surface, which may help transfer of photoinduced electrons from photosensitizers to CdS. The photovoltaic performance of CdS-conjugated polymer photosensitizers was investigated by measuring current density−voltage ($J-V$) characteristics. Figure 4b,c shows typical $J-V$ curves and the IPCE of LM 4 polymer on CdS nanowires/FTO electrodes, respectively. The solid electrochemical cells with LM 4 polymer shows the maximum conversion efficiency (E_{ff}) of 1.73% with a short circuit current (J_{sc}) of −5.26 mA/cm^2, an open-circuit voltage (V_{oc}) of 0.60 V, and a fill factor (ff) of 0.54. CdS nanowire/conjugated polymer photosensitizer solar cells show increased properties compared to CdS nanocrystal/conjugated polymer solar cells,[14] which was considered to attribute to the cell structure bearing one-dimensional nanowires directly connected to the electrode. This improves charge collection efficiency owing to reduced short circuiting and thus increases the shunt resistance and V_{oc}. According to the reasons, to achieve higher efficiency, the synthetic method should be modified to further increase surface area and efficient pathways by growing more vertically aligned nanowires with higher aspect ratio and higher density.

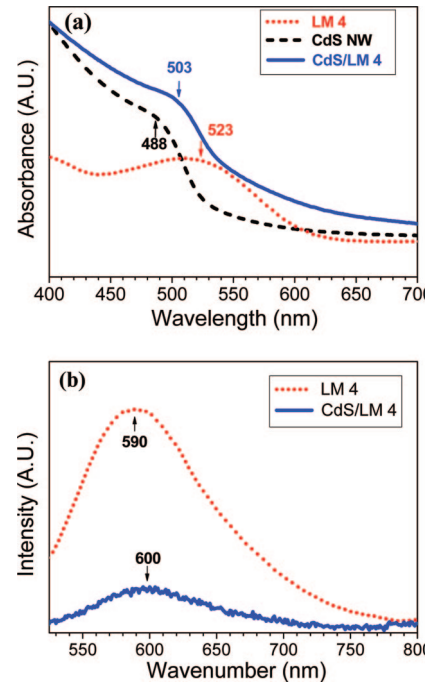

Figure 3. (a) UV−vis light absorption of CdS nanowires, LM 4, and CdS nanowires/LM 4 and (b) photoluminescence (PL) spectra of CdS nanowires/LM 4 and LM 4.

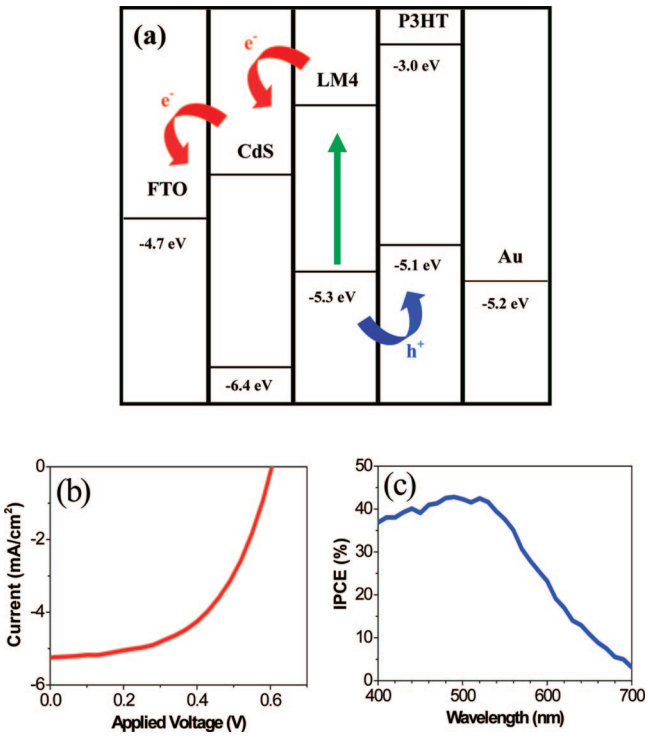

Figure 4. (a) Schematic diagram of energy level for CdS nanowires/LM 4/P3HT solar cell, (b) current−voltage ($J-V$) characteristics, and (c) incident photon-to-current conversion efficiency (IPCE) of CdS nanowires/LM 4/P3HT.

4. Conclusions

To conclude, for the first time high-density and single-crystalline CdS nanowire arrays were successfully synthesized on FTO glass substrates without the aid of templates. Bi was used as a catalyst for SLS growth of CdS nanowires at 220 °C. Resulting nanowires were very straight and vertically grown from the substrates. Control of precursor concentration and temperature played a major role in CdS nanowire growth by preventing precipitation of CdS nanocrystals. PVA coating was a key factor to hold liquid-phase Bi catalysts at the surface of FTO glass substrates during the nucleation and growth of nanowires. Moreover, the potential of the CdS nanowire arrays to be used as photovoltaic cells was demonstrated by fabricating organic−inorganic hybrids of CdS-LM 4-P3HT. The hybrid photovoltaic cells were operated with 1.73% power conversion efficiency. This low-temperature SLS process for the formation of CdS nanowire arrays on a conductive glass substrate can be extended to the formation of other semiconductor nanowire arrays on glass and the development of various low-cost transparent electronic devices becomes possible. Furthermore, owing to the low-temperature processing even polymer films can be employed as a substrate for the growth of semiconductor nanowires that can be used for flexible electronic device applications.

Acknowledgment. This work was supported by the Components and Materials Technology Development Program funded by the Ministry of Knowledge Economy, Republic of Korea (MKE, Korea).

Supporting Information Available: This material is available free of charge via the Internet at http://pubs.acs.org.

References and Notes

(1) Xia, Y. N.; Yang, P. D.; Sun, Y. G.; Wu, Y. Y.; Mayers, B.; Gates, B.; Yin, Y. D.; Kim, F.; Yan, Y. Q. *Adv. Mater.* **2003**, *15*, 353.

(2) (a) Gudkinsen, M. S.; Lauhon, L. J.; Wang, J.; Smith, D. C.; Lieber, C. M. *Nature* **2002**, *415*, 617. (b) Kind, H.; Yan, H. Q.; Messer, B.; Law, M.; Yang, P. D. *Adv. Mater.* **2002**, *14*, 158. (c) Wan, Q.; Li, Q. H.; Chen, Y. J.; Wang, T. H.; He, X. L.; Li, J. P.; Lin, C. L. *Appl. Phys. Lett.* **2004**, *84*, 3654. (d) Cui, Y.; Lieber, C. M. *Science* **2001**, *291*, 851. (e) Yang, X. N.; Loos, J.; Veenstra, S. C.; Verhess, W. J. H.; Wienk, M. M.; Kroon, J. M.; Michels, M. A. J.; Janssen, R. A. J. *Nano Lett.* **2005**, *5*, 579. (f) Nam, K. T.; Kim, D. W.; Yoo, P. J.; Chiang, C. Y.; Meethong, N.; Hammond, P. T.; Chiang, Y. M.; Belcher, A. M. *Science* **2006**, *312*, 885. (g) Lee, J.-C.; Kim, T. G.; Choi, H.-J.; Sung, Y.-M. *Cryst. Growth Des.* **2007**, *7*, 2588. (h) Liao, L.; Lu, H. B.; Li, J. C.; He, H.; Wang, D. F.; Fu, D. J.; Liu, C.; Zhang, W. F. *J. Phys. Chem. C* **2007**, *111*, 1900.

(3) (a) Lee, J.-C.; Kim, T. G.; Choi, H.-J.; Sung, Y.-M. *Appl. Phys. Lett.* **2007**, *91*, 113104. (b) Lee, J.-C.; Kim, T. G.; Choi, H.-J.; Sung, Y.-M. *Nanotechnology* **2006**, *17*, 4317. (c) Persson, A. I.; Larsson, M. W.; Stenstrom, S.; Ohlsson, B. J.; Samuelson, L.; Wallenberg, L. R. *Nat. Mater.* **2004**, *3*, 677.

(4) (a) Song, J.; Lim, S. *J. Phys. Chem. C* **2007**, *111*, 596. (b) Jiang, X. C.; Wang, Y. L.; Herricks, T.; Xia, Y. N. *J. Mater. Chem.* **2004**, *14*, 695.

(5) (a) Huang, M. H.; Mao, S.; Feick, H.; Yan, H. Q.; Wu, Y. Y.; Kind, H.; Weber, E.; Russo, R.; Yang, P. D. *Science* **2002**, *292*, 1897. (b) Huang, M. H.; Wu, Y. Y.; Feick, H.; Tran, N; Weber, E.; Yang, P. D. *Adv. Mater.* **2001**, *13*, 113.

(6) (a) Yu, H.; Li, J. B.; Loomis, R. A.; Gibbson, P. C.; Wang, L. W.; Buhro, W. E. *J. Am. Chem. Soc.* **2003**, *125*, 16168. (b) Sun, J. W.; Buhro, W. E. *Angew. Chem., Int. Ed.* **2008**, *47*, 3215. (c) Sun, J. W.; Buhro, W. E. *J. Am. Chem. Soc.* **2008**, *130*, 7997. (d) Dong, A.; Tang, R.; Buhro, W. E. *J. Am. Chem. Soc.* **2007**, *129*, 12254.

(7) (a) Miao, Z.; Xu, D. S.; Ouyang, J. H.; Guo, G. L.; Zhao, X. S.; Tang, Y. Q. *Nano Lett.* **2002**, *2*, 717. (b) Thurn-Albrecht, T.; Schotter, J.; Kastle, C. A.; Emley, N.; Shibauchi, T.; Krusin-Elbaum, L.; Guarni, K.; Black, C. T.; Tuominen, M. T.; Russell, T. P. *Science* **2000**, 29–2126.

(8) Ouyang, L.; Maher, K. N.; Yu, C. L.; McCarty, J.; Park, H. *J. Am. Chem. Soc.* **2007**, *129*, 133.

(9) Law, M.; Greene, L. E.; Johnson, J. C.; Saykally, R.; Yang, P. D. *Nat. Mater.* **2005**, *4*, 455.

(10) Cao, G. *Nanostructures & Nanomaterials: Synthesis, Properties, and Applications*; Imperial College: London, 2004; p 54.

(11) Cao, G. *Nanostructures & Nanomaterials: Synthesis, Properties, and Applications*; Imperial College: London, 2004; p 130.

(12) Moser, Z.; Dutkiewicz, J.; Zabdyr, L.; Salawa, J. *J. Phase Equilib.* **1988**, *9*, 445.

(13) Shevchenko, E. V.; Talapin, D. V.; Schnablegger, H.; Komowski, A.; Festin, O.; Svedlindh, P.; Haase, M.; Weller, H. *J. Am. Chem. Soc.* **2003**, *125*, 9090.

(14) Wang, L.; Liu, Y. S.; Qin, D. H.; Cao, Y. *J. Phys Chem. C* **2007**, *111*, 9538.

JP809365Z